scientific reports

Check for updates

OPEN

# Enhanced methane production from bloom algal biomass using hydrothermal and hydrothermal-alkaline pretreatment with anaerobic digestion

Zaixing Huang[1,2]✉, Jingzhuo Zhou[1], Yuxiang Zhong[1], Yajie Chang[1], Wanrong Yin[1], Shuzhong Zhao[1], Yi Yan[1], Weiting Zhang[1], Qingfeng Gu[1], Huan He[1]✉, Michael Urynowicz[2], Muhammad Adnan Sabar[3], Gordana Medunić[4], Fang-Jing Liu[1], Hongguang Guo[5], Asif Jamal[6], Muhammad Ishtiaq Ali[6] & Rizwan Haider[7]

**Coalbeds have the potential as geobioreactors for producing renewable natural gas from biomass derived from photosynthesis. This brings about a number of benefits, including support for sustainable energy and the sequestration of carbon dioxide in coal. In this study, freshwater bloom algae were employed as the substrate to examine the influence of hydrothermal and hydrothermal-alkaline pretreatment on methane production using an inoculum from an anaerobic digester. The morphology and chemical structures of the biomass, as well as the volatile fatty acids (VFAs) in the liquid fraction of the post-treatment and gas production, were analyzed to understand their relationship with the efficacy of methane yields and changes in microorganisms. The results revealed that both hydrothermal and hydrothermal-alkaline pretreatment, under the right conditions, can lead to an increase in methane production. Particularly, a pretreatment condition of 0.2 mol/L NaOH at 150 °C for 30 min resulted in a significant increase in methane yield by up to 303.9%. The addition of NaOH facilitated the hydrothermal-alkaline pretreatment, effectively destroying the cell structure of the bloom algae, promoting the dissolution of intracellular sugars and other substances, and reducing the loss of VFAs caused by heating. Moreover, hydrothermal-alkaline pretreatment was found to support the growth of acetoclastic methanogens and enhance methane production by mitigating pH drops. Overall, the results of this study suggest that hydrothermal-alkaline pretreatment offers significant advantages in methane production compared to hydrothermal pretreatment. These findings have important implications for harnessing bloom algae as a viable source for generating renewable natural gas.**

**Keywords** Bloom algae, Anaerobic digestion, Methane, Hydrothermal pretreatment, Hydrothermal-alkaline pretreatment, Renewable natural gas

Although approximately 95% of the vast 21 trillion-ton coal resources are not mineable, they can be explored for many other applications including the production of renewable natural gas with carbon sequestration[1,2]. Photosynthesis-derived biomass including plants and algae has been reported for such endeavors[3–5]. Eutrophication in freshwater can result in excessive growth of algae and the formation of algal bloom, causing

[1]Key Laboratory of Coal Processing and Efficient Utilization of Ministry of Education, School of Chemical Engineering and Technology, China University of Mining and Technology, Xuzhou 221116, China. [2]Department of Civil and Architectural Engineering and Construction Management, University of Wyoming, Laramie, WY 82071, USA. [3]Department of Environmental Engineering, Faculty of Engineering, Chulalongkorn University, Bangkok 10330, Thailand. [4]Department of Geology, Faculty of Science, University of Zagreb, Horvatovac 95, Zagreb 10000, Croatia. [5]College of Safety and Emergency Management and Engineering, Taiyuan University of Technology, Taiyuan 030024, China. [6]Department of Microbiology, Quaid-i-Azam University, Islamabad 44000, Pakistan. [7]Institute of Energy & Environmental Engineering, University of the Punjab, Lahore 54590, Pakistan. ✉email: zhuang@uwyo.edu; hehuan6819@cumt.edu.cn

harm to aquatic organisms due to the reduction in dissolved oxygen and the increase of turbidity[6]. Despite various physical, chemical, and biological methods being deployed to control the occurrence of algal bloom, their efficacy has been inconsistent[7]. Conventional methods are typically associated with intensive labor and high costs[7,8]. On the other hand, algae are widely regarded as a promising source for biofuels because of their highly efficient biological machinery in the conversion of solar energy to biomass[9]. Algae are readily available and not restricted by geographical and seasonal factors[10]. They can fix atmospheric $CO_2$ into carbohydrates, lipids, and proteins with versatile food sources[11]. Therefore, the utilization of algal resources particularly bloom algae for renewable natural gas production has multifaceted environmental and socio-economic benefits.

A range of microalgae have been evaluated for their potential in methane production[12]. Among them, bloom algae have been found to be particularly promising substrates in terms of methane conversion rate. However, the cell walls of algae can impede the dissolution and hydrolysis of intracellular organic matter, such as carbohydrates and proteins, leading to low conversion rates by microorganisms. This has greatly limited the prospects of industrial application[13]. A pretreatment is usually needed in this regard. Previous studies have reported that hydrothermal and chemical methods (acid, alkali) can be used to pretreat microalgae biomass for the production of value-added products[14]. Hydrothermal pretreatment can greatly improve the solubility of microalgae cells, but high temperature can lead to the formation of melanoidin, an inhibitor to anaerobes[15]. Acid and alkaline pretreatment can disrupt cell walls and intracellular components, reducing the polymerization and crystallinity of polymers. However, the effectiveness of these methods depends on cell wall composition and intracellular components of the microalgae species[16,17]. Despite extensive investigation into the anaerobic fermentation of algal biomass in recent years, most studies have focused on a single-factor variable, with multi-factor pretreatment conditions for biogas production being poorly reported. In addition, the effect of pretreatment methods on the subsequent anaerobic processes is also not well understood, limiting the potential for using bloom algae for biomethane production.

The hydrothermal treatment and anaerobic digestion of algal biomass have been extensively studied, with numerous reports highlighting the significant impact of single-factor variables on process efficiency and product yields. Temperature is one of the most influential factors, as it affects the hydrolysis, depolymerization, and solubilization of organic matter. Previous studies have demonstrated that increasing hydrothermal treatment temperatures can enhance the solubilization of algal biomass, leading to higher biogas yields during subsequent anaerobic digestion[18–20]. Similarly, the concentration of biomass and the pH conditions during hydrothermal treatment have been shown to affect the composition and properties of the hydrolysate, which in turn influences the methane production potential[21,22]. In the context of anaerobic digestion, the substrate-to-inoculum ratio is a critical parameter that dictates the microbial activity and stability of the digestion process[23]. Research indicates that an optimal substrate-to-inoculum ratio is essential for maximizing methane production while preventing process inhibition[24]. Additionally, the hydraulic retention time (HRT) and organic loading rate (OLR) are crucial operational parameters that need to be optimized to ensure efficient digestion and high biogas yields[25,26]. The interplay between these single-factor variables underscores the complexity of optimizing hydrothermal treatment and anaerobic digestion processes for algal biomass.

This study aimed to evaluate the potential of using bloom algae as a substrate for methane production with an inoculum sourced from a food brewing facility. The experiments were conducted with various hydrothermal and hydrothermal-alkaline pretreatments, taking into consideration the effects of treatment temperature, duration, and alkaline concentrations. The characteristics of the treated biomass and the liquid fractions were analyzed both before and after gas production of the optimal pretreatment conditions. In addition, the study aimed to shed light on the main treatment parameters responsible for the differences in methane production potential and the reduction in microbial diversity. By exploring the impact of different pretreatment conditions on the bloom algae, the goal of this study was to provide insights that could help improve the production of methane from this renewable source.

## Materials and methods

### Bloom algae and inoculum sources

Bloom algae used in this study were procured from Qingzhi Environmental Protection Technology Company (Xuzhou, China). The algae were cleaned by washing them with water and then centrifuged at 1200 rpm for 10 min. The resulting algae pellet was dried in an oven at 40 °C for 24 h and then mixed thoroughly. Dried algae biomass instead of wet samples was prepared and used to ensure consistency and control over the experimental conditions. Table 1 presents the results of the proximate analysis, ultimate analysis, and nutrient content analysis of the algal sample. An inoculum sample was collected from an anaerobic digester at Xuzhou Wantong Food Brewing Company (Xuzhou, China) and stored in a refrigerator (4 °C) for further use.

### Pretreatment of algae and chemical oxygen demand (COD) analysis

The dried bloom algae were subjected to hydrothermal pretreatment or hydrothermal-alkaline pretreatment. In the hydrothermal pretreatment, the algae were treated at temperatures of 50 °C, 100 °C, and 150 °C for 30 min, 60 min, or 90 min. A total of 9 samples were prepared, as shown in Table 2 (Passos et al., 2016). The sample IDs refer to the number of the sample under each pretreatment method. In the hydrothermal-alkaline pretreatment, NaOH was added to the pretreatment system at concentrations of 0.05 mol/L, 0.1 mol/L, or 0.2 mol/L. Temperatures and treatment times were the same as in the hydrothermal process. An orthogonal experimental design can be used to determine the optimal conditions while minimizing the number of samples[27]. Liu et al. (2022) utilized an orthogonal test design to investigate the frost-heave characteristics of saturated lean clay fillers. An L9 ($3^4$) orthogonal array was applied to allow for the evaluation of four factors at three levels each with only nine experimental runs[28]. This approach facilitated the identification of significant factors and their optimal levels efficiently, demonstrating the method's capability to reduce experimental workload while

| | | |
|---|---|---|
| Proximate analysis | Moisture | 5.88% |
| | Ash | 1.70% |
| | Volatile matter | 88.59% |
| Ultimate analysis | Carbon | 43.48% |
| | Hydrogen | 6.20% |
| | Oxygen | 49.70% |
| | Nitrogen | 0.46% |
| Nutrients | Total polysaccharide | 63.45% |
| | Protein | 7.84% |
| | Grease | 13.58% |

**Table 1**. Proximate, ultimate, and nutrient analysis of bloom algae on an as-received basis.

| Sample IDs | Time (min) | Temperature (°C) |
|---|---|---|
| 1 | 30 | 50 |
| 2 | 30 | 100 |
| 3 | 30 | 150 |
| 4 | 60 | 50 |
| 5 | 60 | 100 |
| 6 | 60 | 150 |
| 7 | 90 | 50 |
| 8 | 90 | 100 |
| 9 | 90 | 150 |

**Table 2**. Experiment conditions of hydrothermal pretreatment.

| Sample IDs | NaOH (mol/L) | Time (min) | Temperature (°C) |
|---|---|---|---|
| 1 | 0.05 | 60 | 150 |
| 2 | 0.05 | 30 | 50 |
| 3 | 0.05 | 90 | 100 |
| 4 | 0.1 | 60 | 50 |
| 5 | 0.1 | 30 | 100 |
| 6 | 0.1 | 90 | 150 |
| 7 | 0.2 | 60 | 100 |
| 8 | 0.2 | 30 | 150 |
| 9 | 0.2 | 90 | 50 |

**Table 3**. Orthogonal experiment design of hydrothermal-alkaline pretreatment.

providing comprehensive insights into the effects of multiple variables. In this study, the same experiment design was employed to independently evaluate the parameters of heating temperature, treatment duration, and NaOH concentrations. A total of 9 setups were prepared, as shown in Table 3. The data collected from the hydrothermal-alkaline pretreatment was analyzed using range analysis to identify the primary and secondary factors affecting the pretreatment[27]. Specifically, a mixture of 1 g pre-dried bloom algae and 50 mL water/alkaline solution was heated in a water bath (50 °C), an autoclave (100 °C), or a pressurized reactor (150 °C) for the designated period. The autoclave (Model: LDZX-30KBS) was manufactured by Shen'an Medical Instrument (Shanghai, China) and is capable of reaching a maximum temperature of 121 °C. The pressurized reactor (Model: YZPR-SS-T3-100-RJ-M-E-N-0-0), manufactured by Yanzheng Instrument (Shanghai, China), has a maximum operating temperature of 350 °C and a maximum pressure capacity of 10 MPa. Serum bottles were used for experiments conducted at 50 °C and 100 °C. A rubber liner was employed within the pressured reactor to hold the materials. The pressure in the autoclave was at ~ 0.14 MPa at 100 °C and reactor stabilized at ~ 0.20 MPa at 150 °C.

To determine the COD of the pretreated samples, the undissolved algal biomass was separated through centrifugation at 1000 rpm for 10 min. The resulting supernatant was then filtered with a 0.22 μm membrane filter (Sangon Biotech, Shanghai, China) and diluted with deionized water to a desired concentration. The COD analysis was performed using a COD analyzer (5B-3 F, Lianhua Technology, Beijing, China) in accordance with the standard method[29]. Briefly, the filtered sample was added to the COD vial containing potassium dichromate

and digested at 150 °C for 2 h. After cooling down, the vial was wiped and placed in the COD analyzer for COD measurement.

## Microcosm preparation and headspace gas analysis

Microcosms were set up in an anaerobic chamber aseptically using 250-mL serum bottles. Each bottle contained 50 ml of an algal sample and 20 mL of a mineral solution. The final concentrations of minerals in g/L were as follows[30]: $MgCl_2$ 0.2, KCl 0.4, NaCl 1, $NH_4Cl$ 2. The pH of the mixture was adjusted to 7.0 ± 0.1 with 1 mol/L HCl and KOH solutions. The inoculum was prepared by diluting 200 g sludge with 1000 mL of deionized water. The clear fraction of the diluent was used as the inoculum. Then, an aliquot of 10 mL inoculum was added to each microcosm and sealed. Bottles containing inocula and mineral solution but no substrate served as negative controls (The negative controls did not have any methane detected and were not shown in the results). The samples were prepared in triplicate. Microcosms were incubated at 35 °C for 69 days.

The headspace gas was analyzed with a Trace 1300 gas chromatograph (GC, Thermo Scientific, Waltham, USA) equipped with a thermal conductivity detector (TCD) and a TracePLOT TG-BOND Sieve 5 A column (Thermo Scientific, Waltham, USA) with a dimension of 30 m × 0.53 mm. The injection and oven temperatures were 100 °C and 60 °C, with the auxiliary heater temperature at 80 °C. The sample was run using high-purity $N_2$ as the carrier gas at a flow rate of 1 mL/min.

The cumulative methane production was estimated using the Gompertz model[31]. The equation is given by:

$$y = A * exp\left\{-exp\left[\left(\frac{\mu_m * exp}{A} * (\lambda - t) + 1\right)\right]\right\}$$

where y is the methane yield; A is the methane potential; $\mu_m$ is the growth rate; λ is the lag time, and t is the incubation time. The model was used to estimate the methane yield for the control, hydrothermal and hydrothermal-alkaline pretreatment.

## Fourier transform infrared (FT-IR) spectroscopy and field emission scanning electron microscope (FE-SEM) analysis

FT-IR and FE-SEM analysis were conducted on the algal samples before and after gas production. The samples were centrifuged at 3000 rpm for 10 min. The supernatant was transferred and stored in a refrigerator for further analysis. The pellet was dried in an oven at 40 °C for 24 h. 0.05 g of the algae was mixed with 5 g KBr and pressed into a pellet for FT-IR (VERTEX 80v, Bruker, Düsseldorf, Germany) analysis. 14 scans were run in the range of 400–4000 $cm^{-1}$ with a resolution of 2 $cm^{-1}$. Morphological analysis was performed using a Zeiss Gemini SEM 500 FE-SEM (Braunschweig, Germany). The algal sample was spread on a conductive tape and coated with gold before being analyzed at a working voltage of 2 kV.

## VFAs and pH analysis

The liquid samples collected before (after pretreatment), during (day 20), and after gas production were filtered with 0.45 µm filters and analyzed with an Agilent HPLC system (1260 Infinity II, Agilent, California, USA) equipped with an Ultimate AQ-C18 column (4.6×250 mm, 5 µm, Agilent, California, USA). Two eluent solutions were employed, consisting of 20 mM $KH_2PO_4$ at pH 2.5 (Solution A) and methanol (Solution B). The sample was run with a gradient of the A and B solutions initially at A: 100% and B: 0% to A: 0% and B: 100% after 20 min elution time at a fixed flow rate of 0.7 mL/min and a column temperature of 30 °C. The injection volume of the sample was 10 µL. The data were acquired at a wavelength of 210 nm. HPLC-grade of oxalic acid ($C_2H_2O$), tartaric acid ($C_4H_6O_6$), formic acid ($CH_2O_2$), malic acid ($C_4H_6O_5$), lactic acid ($C_3H_6O_3$), acetic acid ($C_2H_4O_2$), citric acid ($C_6H_8O_7$), and succinic acid ($C_4H_6O_4$) were used for calibration. The pH of the sample was determined using a desktop digital pH meter (PHS-3E, Leici, Shanghai, China).

## DNA extraction and sequencing

DNA of the inoculum and microorganisms from exponential gas production microcosms at day 40 was extracted with an E.Z.N.A.® soil DNA kit (Omega Bio-Tek, Norcross, GA, USA) according to manufacturer's instructions. The DNA concentration and quality were determined by a spectrophotometer (UV-2600i, SHIMADZU, Tokyo, Japan) and agarose gel electrophoresis. The 16S rRNA genes of bacteria were amplified using primer sequences 338F (ACTCCTACGGGAGGCAGCAG) and 806R (GGACTACHVGGGTWTCTA-AT)[32]. The 16S rRNA genes of Archaea were amplified using primer sequences 524F10extF (TGYCAGCCGCCGCGGTA-A) and arch958RmodR (YCCGGC-GTT-GAVTCCAATT)[33]. The purified PCR amplicons were combined in equimolar and paired-end sequenced (2 × 300) on an Illumina Miseq platform (Illumina, San Diego, USA) at Majio Bioinformatics Technology Co., Ltd. (Shanghai, China), and submitted to NCBI with accession numbers of SRR24982407, SRR24982409, SRR2492410, SRR25016625, SRR25016622, SRR25016627. The data were analyzed on Majorbio Cloud Platform (www.majorbio.com).

## Data analysis

The correlations between chemical oxygen demand and pretreatment conditions as well as methane production and pretreatment conditions were analyzed by regression analysis and bivariate correlation Pearson analysis[27]. Range analysis of the orthogonal test was conducted to access the influence of treatment conditions on COD in the hydrothermal-alkaline pretreatment. The influence of various conditions on methane production in the hydrothermal-alkaline pretreatment was analyzed using the range analysis and variance analysis of the orthogonal test[27]. Pearson correlation coefficient analysis was employed to elucidate the correlation between the sum of formic acid, acetic acid and oxalic acid concentrations and methane production.

## Results

### COD analysis

COD analysis was conducted as an indirect measurement of oxidizable organics after hydrothermal and hydrothermal-alkaline pretreatments, as shown in Fig. 1. In the hydrothermal pretreatment, the results showed an increase in COD for all samples, ranging from 17.6 to 51.26% compared to the control. The COD was positively correlated with the pretreatment time at each temperature with a highly correlated coefficient (e.g., Pearson $\rho = 0.998$ and $R^2 = 0.9968$ for 50 °C, Pearson $\rho = 0.985$ and $R^2 = 0.9697$ for 100 °C, Pearson $\rho = 0.982$ and $R^2 = 0.9641$ for 150 °C). Samples pretreated at 100 °C showed higher COD values than those treated at other temperatures.

For the hydrothermal-alkaline pretreatment, the results of COD were mixed, with some samples showing a marginal increase (2.56% ~17.59%) and others showing a reduction. Both hydrothermal and hydrothermal-alkaline pretreatments could effectively disrupt the microalgal cell structure, facilitating the release and solubilization of intracellular substances[34,35]. This led to an increase in COD after pretreatment. Range analysis indicating the impact each factor had on the COD value is shown in Table 4. It clearly shows that the contribution of these factors was in the order of NaOH concentration ($R = 3029$) > temperature ($R = 622$) > time ($R = 506$). The COD decreased with increasing NaOH concentration.

### Methane production

Methane production was monitored in the headspace of the microcosms for 69 days. The final gas yields of all treatments are shown in Fig. 2. The impact of the pretreatment on the final gas yield varied for both hydrothermal and hydrothermal-alkaline pretreatments when compared to controls (766.9 μmol/g algae).

For the hydrothermal pretreatment, the effect of treatment temperature on the final gas yield was dependent on the treatment time. Short treatment times (30 min) resulted in an increase in gas yield with increasing temperature, with a 25.9% increase observed at 30 min and 150 °C. However, for prolonged treatment times (60 and 90 min), the increase in treatment temperature could reduce the final gas yield by as much as 56% (90 min, 150 °C). For the low treatment temperature (50 °C), an increase in treatment time can improve the yield by as much as 12.7% (90 min, 50 °C). In contrast, high-temperature treatments (100 and 150 °C) resulted in a reduction in gas yield with prolonged treatment time, with the higher temperature and longer time the most. This suggests that high temperatures modify the structures of some compounds, making them less available to microorganisms.

Table 5 presents the range analysis (represented by R values) and variance analysis of the orthogonal test results of the hydrothermal-alkaline pretreatment samples. In the hydrothermal alkaline pretreatment, the highest methane production, i.e., 3097.2 μmol/g, was achieved with a NaOH concentration of 0.2 mol/L, a treatment time of 30 min, and a treatment temperature of 150 °C. For the hydrothermal alkaline pretreatment, the range analysis results of orthogonal design indicate that NaOH concentration ($R = 1616.3$) had the highest contribution to methane production, followed by treatment time ($R = 1068.3$) and temperature ($R = 1034.2$), as

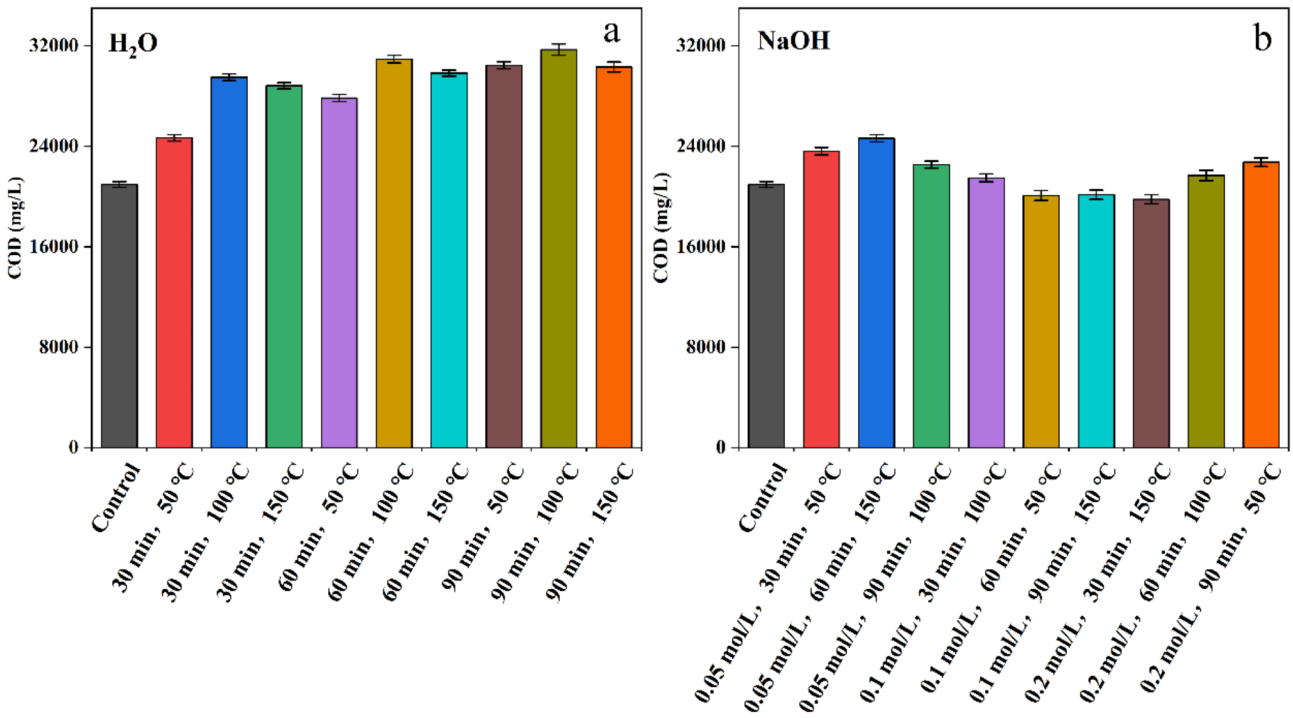


**Fig. 1**. COD of bloom algae under different pretreatment conditions. Data points represent the means ± s.d., $n = 3$ per group.

| Sample IDs | Influencing factors | | | COD (mg/L) |
|---|---|---|---|---|
| | NaOH (mol/L) | Time (min) | Temperature (℃) | |
| 1 | 0.05 | 60 | 150 | 24,644 |
| 2 | 0.05 | 30 | 50 | 23,616 |
| 3 | 0.05 | 90 | 100 | 22,542 |
| 4 | 0.1 | 60 | 50 | 20,079 |
| 5 | 0.1 | 30 | 100 | 21,494 |
| 6 | 0.1 | 90 | 150 | 20,142 |
| 7 | 0.2 | 60 | 100 | 21,684 |
| 8 | 0.2 | 30 | 150 | 19,779 |
| 9 | 0.2 | 90 | 50 | 22,736 |
| $K_1$ | 70,802 | 64,889 | 66,431 | |
| $K_2$ | 61,715 | 66,407 | 65,720 | |
| $K_3$ | 64,199 | 65,420 | 64,565 | |
| $k_1$ | 23,601 | 21,630 | 22,144 | |
| $k_2$ | 20,572 | 22,136 | 21,907 | |
| $k_3$ | 21,400 | 21,807 | 21,522 | |
| R | 3029 | 506 | 622 | |

**Table 4**. Range analysis of orthogonal test results of COD in hydrothermal-alkaline pretreatment.

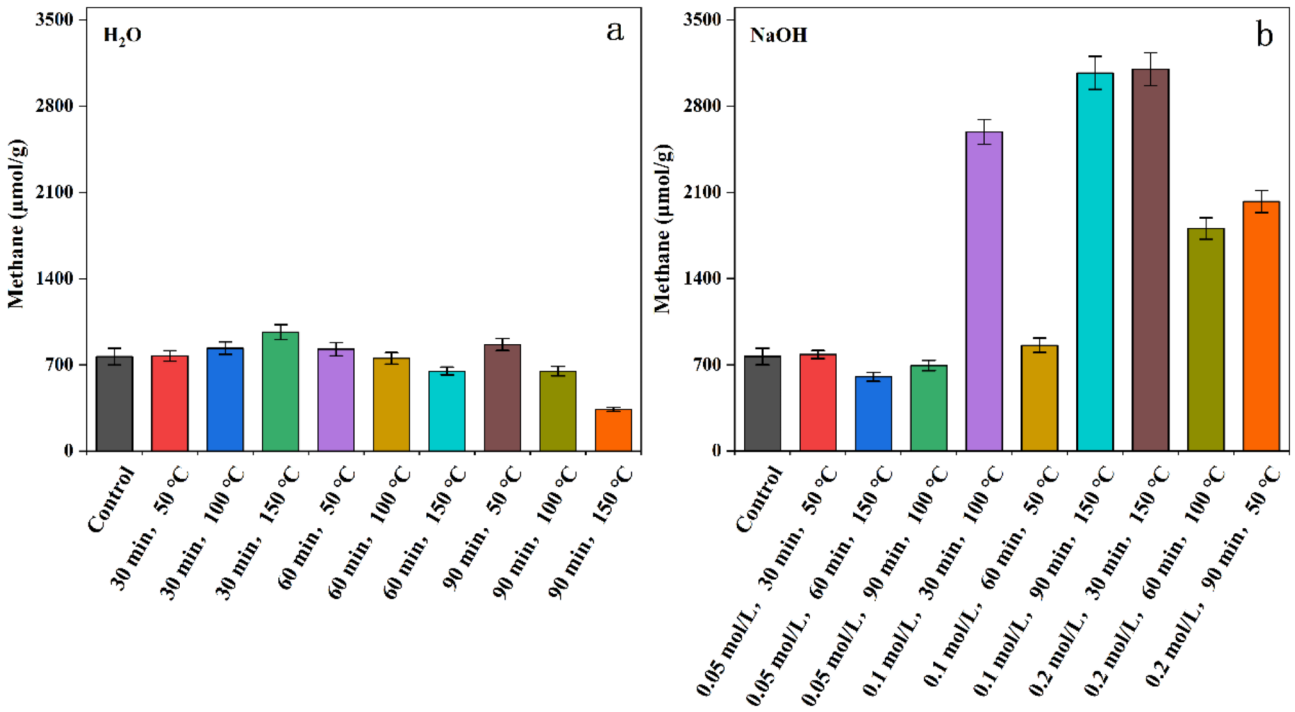


**Fig. 2**. Methane yields at different pretreatment conditions. Data points represent the means ± s.d., $n = 3$ per group.

shown in Table 5. In mathematical terms, these differences are sufficiently significant to determine that NaOH concentration is the main contributor. Furthermore, the results of variance analysis (Table 6) reveal that NaOH concentration as an influencing factor had a significant impact on methane production ($P = 0.034 < 0.05$). The study found that methane production increased exponentially with increasing NaOH concentration ($R^2 = 0.8135$), particularly in the low concentration regime from 0.05 to 0.1 mol/L. Additionally, a linear positive correlation was observed between methane production and temperature (Pearson $\rho = 0.999$, $R^2 = 0.9977$). The highest methane yield of 3097.2 μmol/g algae was obtained under the conditions of 0.2 mol/L NaOH, 30 min, 150 °C, followed by treatments at 0.1 mol/L NaOH, 90 min, 150 °C (3067.8 μmol/g algae) and 0.1 mol/L NaOH, 30 min, 100 °C (2588.4 μmol/g algae), all performed at high temperatures. Similarly, principal component analysis (PCA) demonstrated that sodium hydroxide had the highest positive loading on PCA1 (43.79%), indicating a

| Sample IDs | Influencing factors | | | Methane (μmol/g) |
|---|---|---|---|---|
| | NaOH (mol/L) | Time (min) | Temperature (℃) | |
| 1 | 0.05 | 60 | 150 | 601.8 |
| 2 | 0.05 | 30 | 50 | 783.1 |
| 3 | 0.05 | 90 | 100 | 693.2 |
| 4 | 0.1 | 60 | 50 | 856.7 |
| 5 | 0.1 | 30 | 100 | 2588.4 |
| 6 | 0.1 | 90 | 150 | 3067.8 |
| 7 | 0.2 | 60 | 100 | 1805.4 |
| 8 | 0.2 | 30 | 150 | 3097.2 |
| 9 | 0.2 | 90 | 50 | 2024.4 |
| $K_1$ | 2078.1 | 6468.7 | 3664.2 | |
| $K_2$ | 6512.9 | 3263.9 | 5087.0 | |
| $K_3$ | 6927.0 | 5785.4 | 6766.8 | |
| $k_1$ | 692.7 | 2156.2 | 1221.4 | |
| $k_2$ | 2171.0 | 1088.0 | 1695.7 | |
| $k_3$ | 2309.0 | 1928.5 | 2255.6 | |
| R | 1616.3 | 1068.3 | 1034.2 | |

**Table 5**. Range analysis of orthogonal test results of methane production in hydrothermal-alkaline pretreatment.

| Source of variance | Sum of squares | Degree of freedom | Mean square | F value | *P* value |
|---|---|---|---|---|---|
| A (NaOH) | 4,816,751 | 2 | 2,408,376 | 28.23 | 0.034* |
| B (time) | 1,899,512 | 2 | 949,756 | 11.13 | 0.082 |
| C (temperature) | 1,608,024 | 2 | 804,012 | 9.42 | 0.096 |
| Error | 170,627 | 2 | 85,313 | | |
| Sum | 8,494,913 | 8 | | | |

**Table 6**. ANOVA of orthogonal test results of methane production in hydrothermal-alkaline pretreatment group. *$P < 0.05$ indicates significant correlation.

strong positive correlation with this principal component (Fig. 3). Furthermore, the close proximity of NaOH concentration and methane in the scatter plot suggests a notable correlation between these two variables. It was determined that the optimal conditions for the highest theoretical gas production were 0.2 mol/L NaOH, 30 min, 150 °C, which was confirmed by the sample prepared.

Each treatment of hydrothermal and hydrothermal-alkaline pretreatments as well as the control with the highest cumulative methane production over time and their corresponding Gompertz model fittings are presented in Fig. 4. The gas production data fitted well to the Gompertz model with an $R^2$ of ~ 0.99, as indicated in Table 7. The gas yields estimated by the model are consistent with the actual gas production. The treatment has a minimal effect on the start of gas production, with a lag phase of ~ 17 days. Nonetheless, the maximum specific gas rate (168.7 μmol/g algae/day) of the hydrothermal-alkaline pretreatment was significantly higher than both the hydrothermal pretreatment and control. It is noteworthy that the pretreatment time and temperature of the hydrothermal and hydrothermal-alkaline pretreatments with the highest methane yields were the same (30 min and 150 °C), suggesting that increasing the pretreatment time at high temperatures is not necessary.

## FE-SEM analysis

The microstructure of algae before and after pretreatment, as well as after biodegradation, was studied using FE-SEM. The samples with the highest methane production in each pretreatment (30 min, 150 °C for hydrothermal pretreatment and 0.2 mol/L NaOH, 30 min, 150 °C for hydrothermal-alkaline pretreatment) were selected for the analysis, as depicted in Fig. 5. Algae before pretreatment exhibited a relatively smooth surface (Fig. 5a). After pretreatment, the roughness of the algae increased, with distinct morphology for the two pretreatment methods. The hydrothermal pretreatment resulted in a finer porous structure on the surface, while the algae treated by hydrothermal-alkaline agents resembled a scale-like structure. These differences can be attributed to the different pretreatment mechanisms. However, only minimal amounts of algal residues were recovered after alkaline treatments (e.g. 0.02 mg for 0.2 M NaOH treatment), suggesting the main components contributing to methane production were in the liquid fraction.

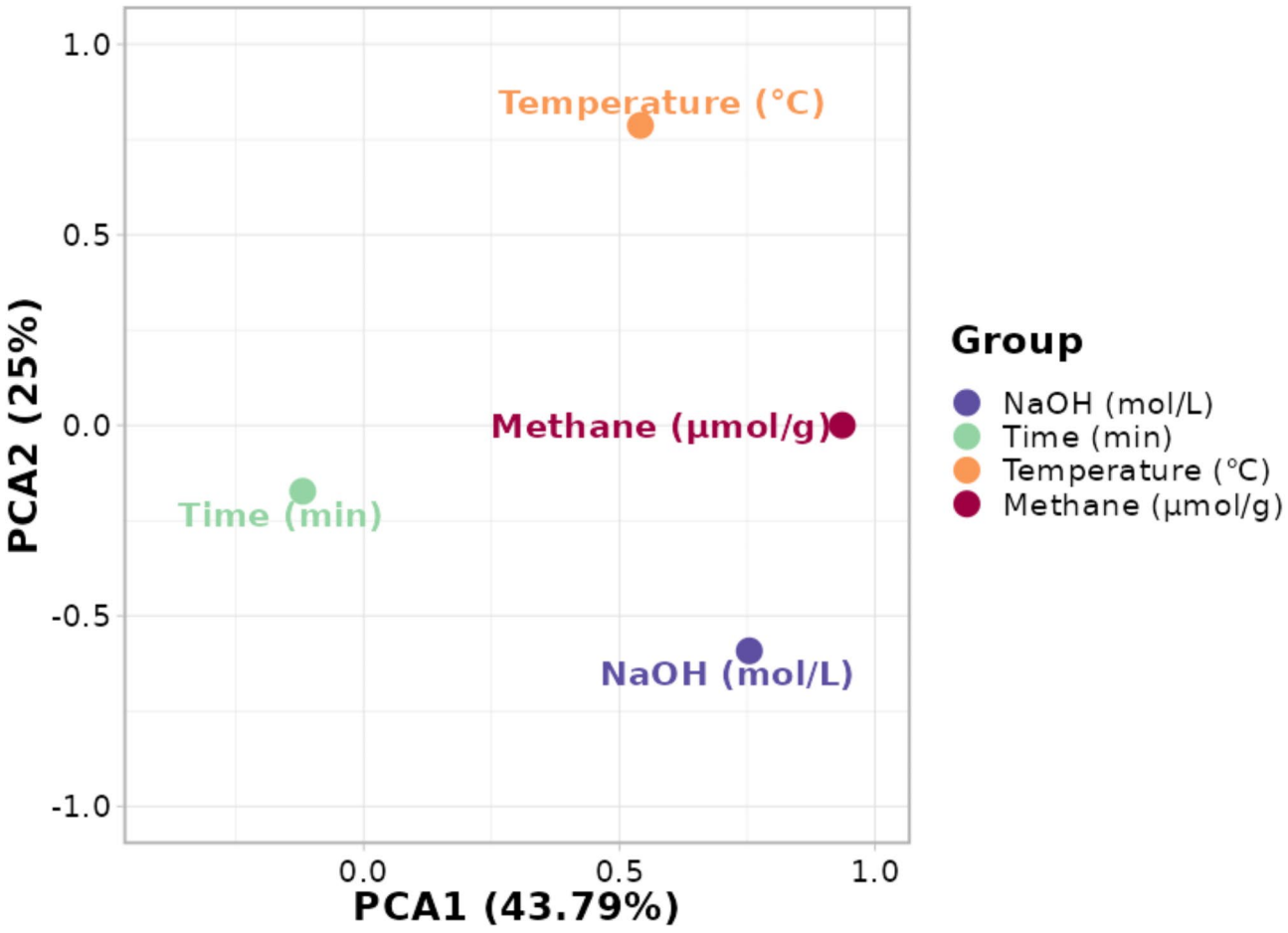


**Fig. 3**. Principal component analysis (PCA) of factors affecting methane yield.

## FT-IR analysis

The samples used in FE-SEM analysis, including 30 min, 150 °C for hydrothermal pretreatment, 0.2 mol/L NaOH, 30 min, 150 °C for hydrothermal-alkaline pretreatment, and untreated control, were also subjected to FT-IR analyses. As shown in Fig. 6, the stretching vibration peaks were mainly observed in the regions of 3750 ~ 2800 $cm^{-1}$ and 1800 ~ 500 $cm^{-1}$. The broad peak with strong absorption at 3750 ~ 3000 $cm^{-1}$ can be attributed to the combination of -OH and amide N-H stretching vibrations[36]. This agrees well with the composition analysis of the algae (Table 1), which were rich in reducing sugars, acids, alcohols, and proteins, bearing abundant -OH and N-H bonds. In comparison to the control and hydrothermal pretreatment samples, the peak intensity in the hydrothermal-alkaline pretreatment sample was higher, suggesting an increased dissolution of reducing sugars, acids, alcohols, and proteins. As these compounds are readily available to microorganisms, the peak intensity was reduced after gas production. The peaks near 2925 $cm^{-1}$ and 2850 $cm^{-1}$ were ascribed to the symmetric and asymmetric C-H stretching vibrations from the methylene functional group of aliphatic compounds associated with fatty acids in algae lipids[37].

In the 1800 ~ 500 $cm^{-1}$ region, multiple peaks were detected. There was a peak at 1651 $cm^{-1}$ in all samples, representing the C = O structure[38]. To be noted, the peak with strong adsorption at 1591 $cm^{-1}$ assigned to C = C in aromatic rings, $-NH_2$ and $-NO_2$ was only observed in the sample of hydrothermal-alkaline pretreatment[39,40]. This was not found in any other samples, suggesting that the hydrothermal-alkaline pretreatment liberated biodegradable moieties. In the 1400 ~ 1200 $cm^{-1}$ band, the samples before biodegradation had absorption peaks, which were signature absorption peaks of sugars[37]. The peaks at 1395 and 1365 $cm^{-1}$ represented C-O stretching vibration in uronic acid[40]. The peak at 1022 $cm^{-1}$ represented C-O-C vibration in the pyranose ring[41]. The intensity was significantly reduced in the control and pretreated samples after gas production.

## VFAs and pH analysis

VFAs and pH levels of the microcosms were determined for hydrothermal-alkaline pretreatment (0.2 mol / L NaOH, 30 min, 150 °C), hydrothermal pretreatment (30 min, 150 °C), and untreated samples (control). The individual VFA, total VFAs, and pH are presented in Figs. 7 and 8. A total of 8 VFAs were identified, including formic acid (C1), acetic acid (C2), oxalic acid (C2), lactic acid (C3), tartaric acid (C4), malic acid (C4), succinic acid (C4), and citric acid (C6). The total VFAs before biodegradation were 108.7 mM for control, 135.7 mM for hydrothermal pretreatment, and 202.3 mM for hydrothermal-alkaline pretreatment. The VFAs were dominated

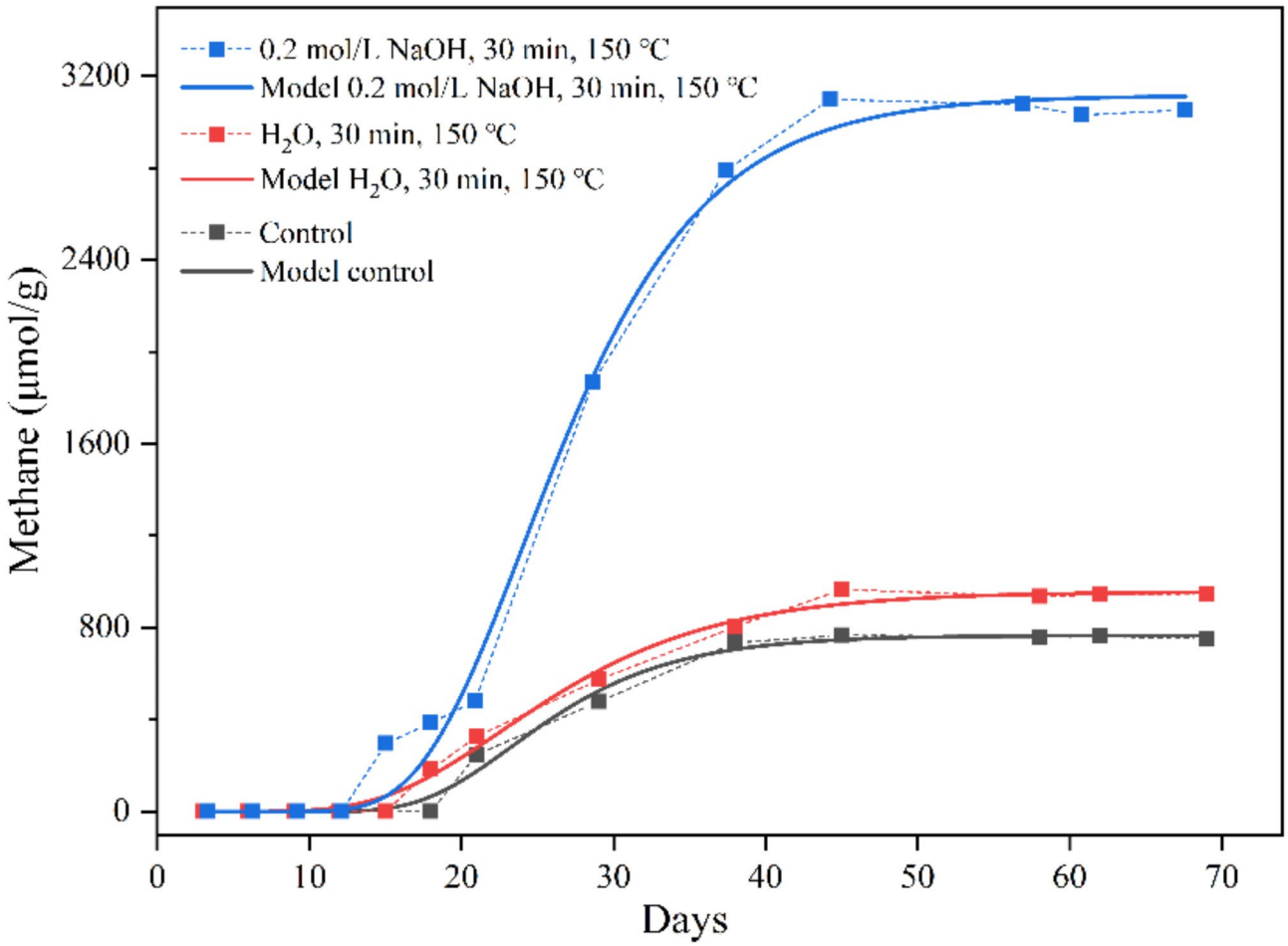


**Fig. 4**. Cumulative methane production and Gompertz model fitting for the hydrothermal (30 min, 150 °C), hydrothermal-alkaline pretreatment (0.2 mol/L NaOH, 30 min, 150 °C), and control. Data points represent the means ± s.d., $n = 3$ per group.

| Treatment/Control | A (μmol/g algae) | $\mu_m$ (μmol/g algae/day) | λ (day) | $R^2$ |
|---|---|---|---|---|
| 0.2 mol/L NaOH, 30 min, 150 °C | 3115.7 (± 62.8) | 168.7 | 16.8 | 0.993 |
| $H_2O$, 30 min, 150 °C | 956.9 (± 22.3) | 50.5 | 17.2 | 0.992 |
| Control | 766.5 (± 19.2) | 47.1 | 17.1 | 0.989 |

**Table 7**. Kinetic parameters and fitting evaluated with the Gompertz model.

by oxalic and malic acids before gas production for control, while in the treated samples, it was mainly composed of VFAs with higher carbon numbers (C4-C6). This suggests that the pretreatment has changed the chemical makeup of algae, which was also confirmed in FT-IR analysis[42].

All microcosms experienced a decrease in pH during the first 20 days of incubation, i.e., 5.4 for control, 5.7 for hydrothermal pretreatment, and 6.3 for hydrothermal-alkaline pretreatment, all below the optimal range of 6.5–7.2[43]. The rapid degradation and formation of VFAs contributed to the reduction in pH[4]. However, methanogens were not suppressed. Instead, exponential gas production was observed thereafter. The total VFAs were reduced by 43.9% for the control, 66.7% for hydrothermal pretreatment, and 94.9% for hydrothermal-alkaline pretreatment. The consumption of these VFAs may greatly account for the increase in pH in the microcosms at the later stage of incubation.

## Microbial analysis

Microcosms of hydrothermal pretreatment (30 min, 150 °C) and hydrothermal-alkaline pretreatment (0.2 mol/L NaOH, 30 min, 150 °C) on day 40 (exponential phases of gas production for all samples), as well as the original inoculum, were selected for microbial analysis, as shown in Fig. 9. The sequences were classified into different taxonomic levels based on the minimum number of sample sequences. A total of 38 phyla, 95 classes, 205 orders,

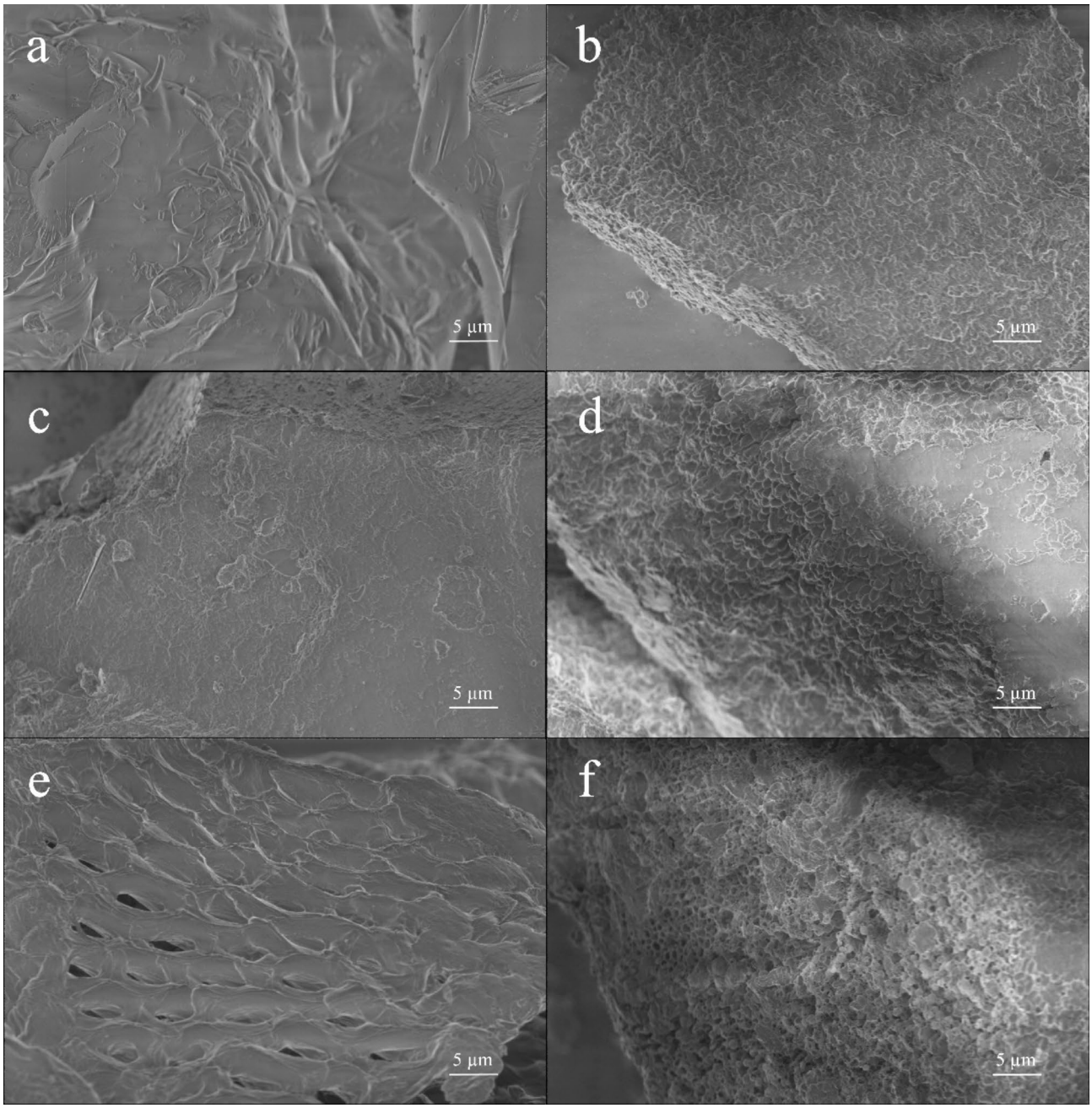


**Fig. 5**. FE-SEM micrographs of bloom algae under different pretreatment conditions and after biodegradation: (**a**) control; (**b**) control after biodegradation; (**c**) hydrothermal pretreatment; (**d**) hydrothermal pretreatment after biodegradation; (**e**) hydrothermal-alkaline pretreatment; (**f**) hydrothermal-alkaline pretreatment after biodegradation.

321 families, and 489 genera of bacteria, and 7 phyla, 11 classes, 12 orders, 16 families, and 22 genera of archaea were annotated in this study.

Table 8 provides an overview of some commonly used metrics of the alpha diversity of bacteria and archaea in hydrothermal, hydrothermal-alkaline pretreatments and the original inoculum. As an indicator of species richness and evenness, the Shannon index of the original inoculum for both bacteria and archaea is the greatest while the Simpson index is the smallest. These suggest that the diversity of the original inoculum was greater than the treated samples[44]. This can be attributed to the limited range of bioavailable substrates in the bloom algae compared to the sludge in the anaerobic digester where the inoculum was sampled.

Figure 9 (a & b) shows the composition of bacteria at phylum and genus levels. In the original inoculum, the dominant phyla were Proteobacteria (39.2%), Bacteroidota (17.4%), and Actinobacteriota (14.1%). The hydrothermal pretreatment (T_1) was dominated by Firmicutes (93.2%) and Proteobacteria (6.7%), while in hydrothermal-alkaline pretreatment (T_2), Bacteroidota (74.9%) was the dominant phylum, followed by

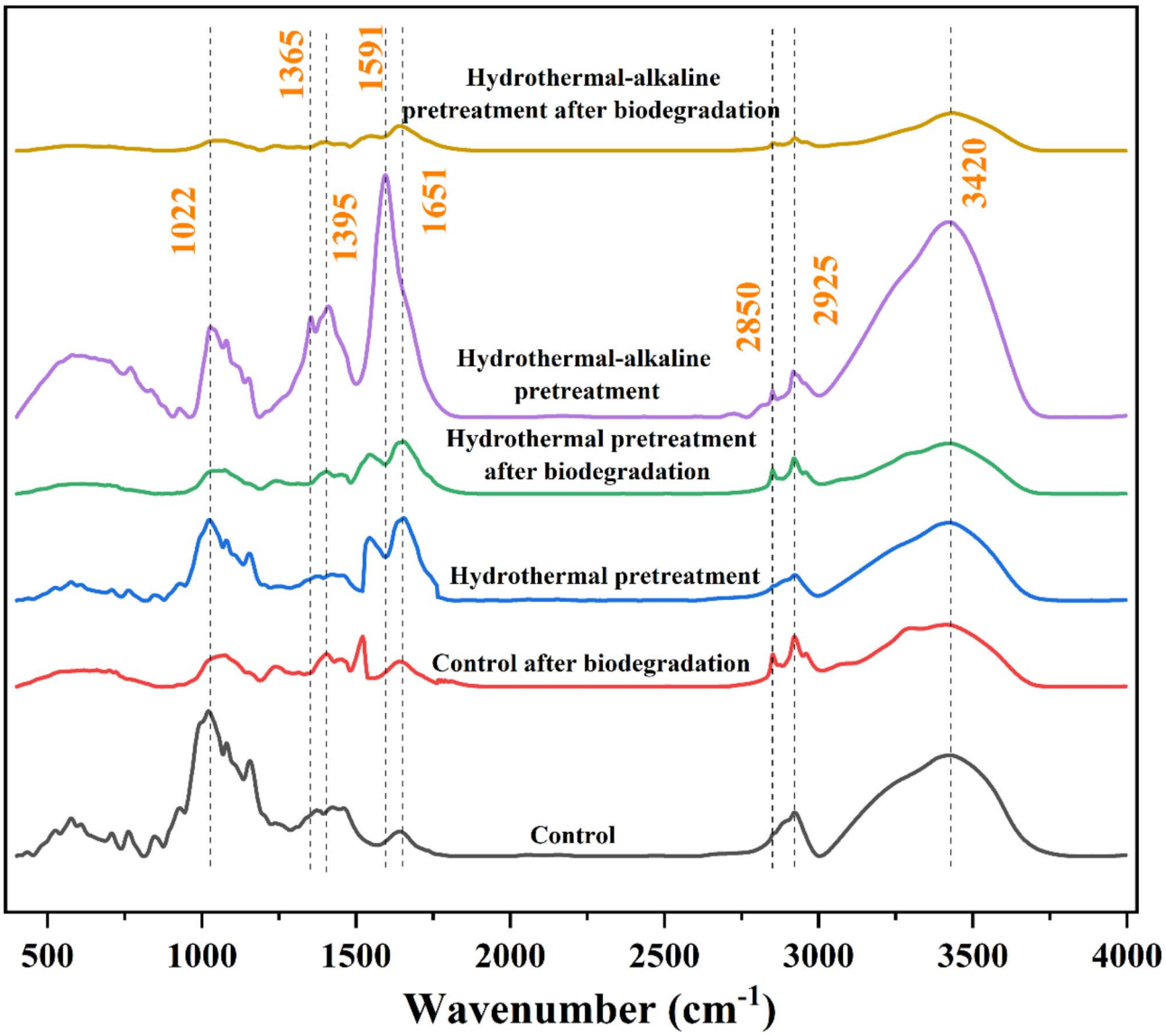


**Fig. 6**. FT-IR analysis of algae after pretreatment and biodegradation.

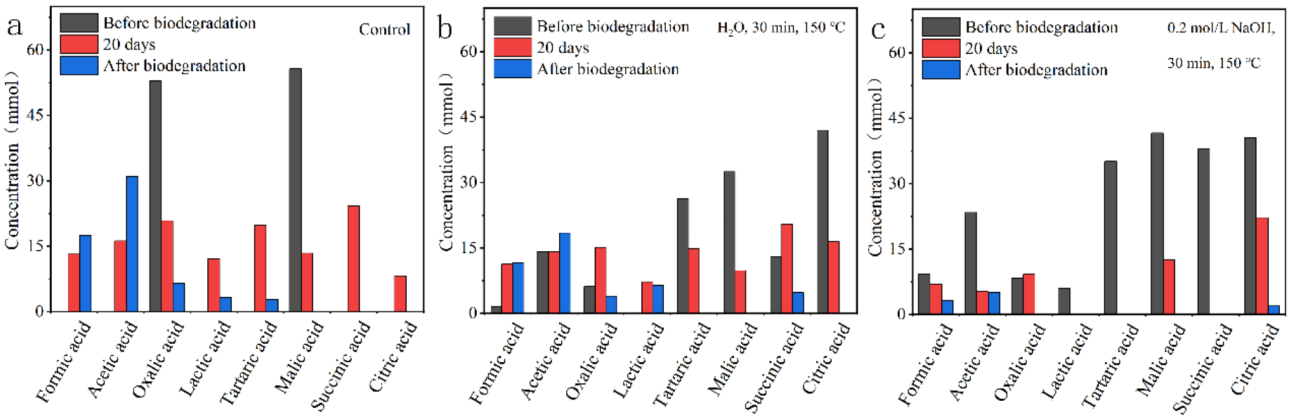


**Fig. 7**. Volatile fatty acids in microcosms. (**a**) Control; (**b**) hydrothermal pretreatment, 30 min, 150 °C; (**c**) hydrothermal-alkaline pretreatment, 0.2 mol/L NaOH, 30 min, 150 °C.

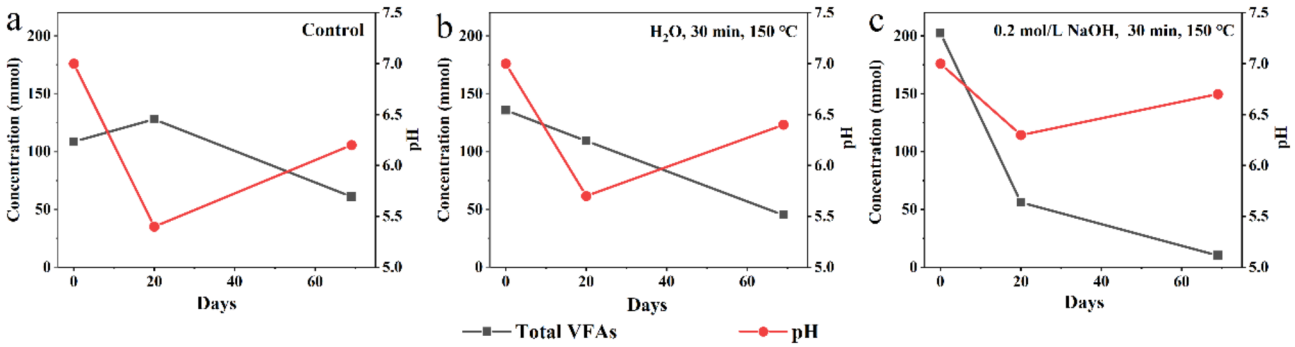


**Fig. 8**. Total volatile fatty acids and pH at sampling intervals of 0, 20 and 69 days. Each data point represents a mean of three replicates. (**a**) Control; (**b**) hydrothermal pretreatment, 30 min, 150 °C; (**c**) hydrothermal-alkaline pretreatment, 0.2 mol/L NaOH, 30 min, 150 °C.

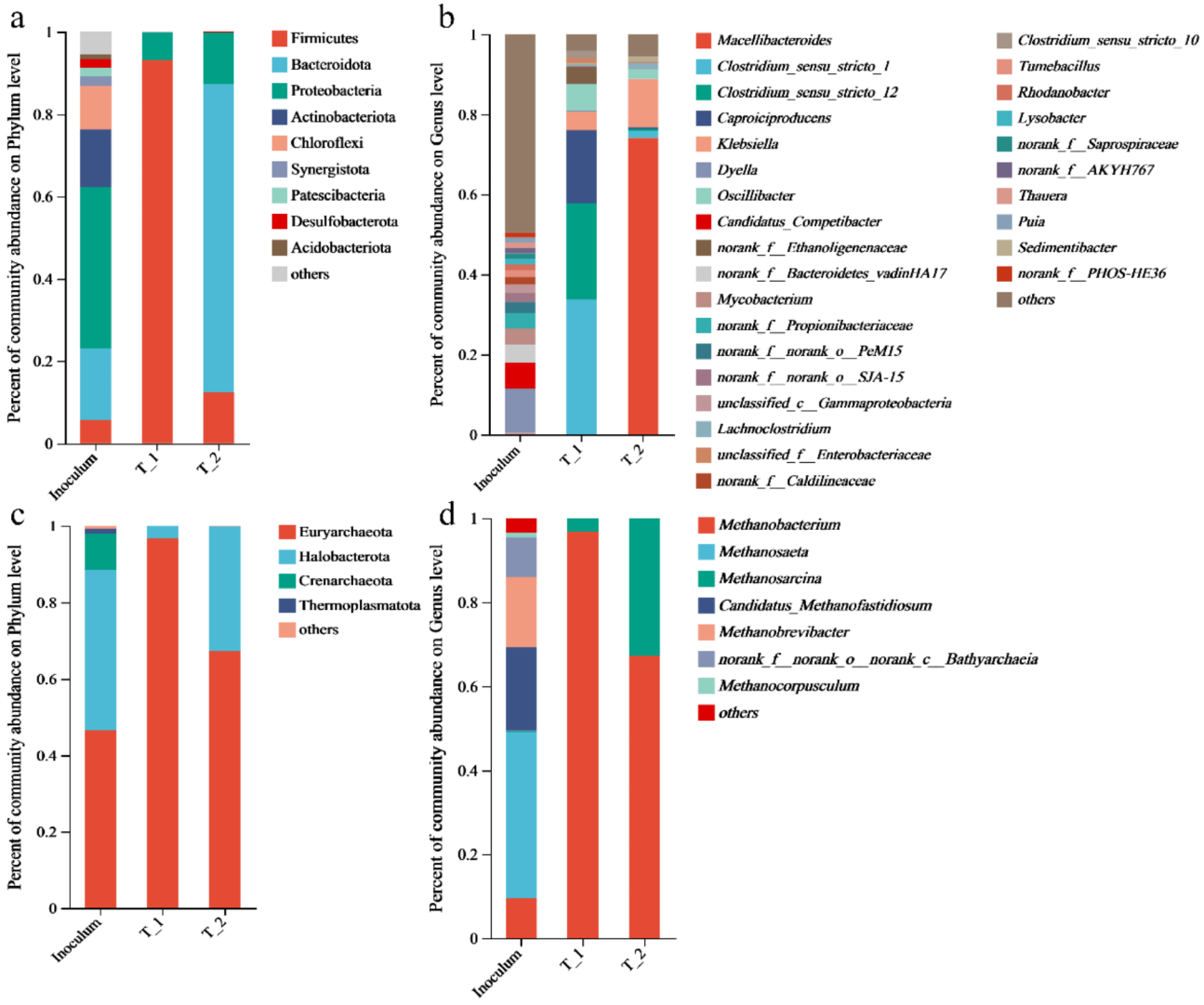


**Fig. 9**. The microbial composition of bacteria (**a**,**b**) and archaea (c and d) at phylum and genus levels at 40 days (exponential phases of gas production). T_1 represents hydrothermal pretreatment (30 min, 150 °C). T_2 represents hydrothermal-alkaline pretreatment (0.2 mol/L NaOH, 30 min, 150 °C).

| Sample | Bacteria | | | | Archaea | | | |
|---|---|---|---|---|---|---|---|---|
| | Chao | Ace | Shannon | Simpson | Chao | Ace | Shannon | Simpson |
| Inoculum | 871.6 | 874.8 | 5.3 | 0.02 | 30.0 | 30.0 | 1.9 | 0.22 |
| T_1 | 140.1 | 142.5 | 2.4 | 0.18 | 3.0 | 0.1 | 0.3 | 0.87 |
| T_2 | 129.1 | 138.5 | 1.2 | 0.56 | 6.0 | 6.0 | 0.6 | 0.56 |

**Table 8**. Indices of alpha diversity of microcosms, T_1: hydrothermal pretreatment (30 min, 150 °C) and T_2: hydrothermal-alkaline pretreatment (0.2 mol/L NaOH, 30 min, 150 °C).

Proteobacteria (12.6%) and Firmicutes (12.4%). At the genus level, *Dyella* (11.1%) was the dominant genus in the inoculum, capable of hydrolyzing and fermenting cellulose and cellobiose[45]. The dominant genera in the hydrothermal pretreatment were *Clostridium_sensu_stricto_1*, *Clostridium_sensu_stricto_12*, and *Caproiciproducens*, representing 75.9% of the OTUs when combined. *Clostridium_sensu_stricto_1* (33.8%) and *Clostridium_sensu_stricto_12* (23.9%) are ubiquitous acid-producing bacteria[46]. *Caproiciproducens* (18.2%), belonging to Firmicutes, can degrade glucose, xylose, and galactose to produce ethanol, VFAs, and other metabolites[47–49]. In the hydrothermal-alkaline pretreatment, *Macellibacteroides* (74.1%) and *Klebsiella* (12.1%) were the dominant genera. The former plays an important role in acid production with acetic acid and butyric acid as the main products[50], while the latter also plays an important role in the acid production process with acetic and succinic acids as the main products[51,52]. In a study, *Macellibacteroides* have shown a strong positive correlation with $Na^+$ concentration[52]. Under $Na^+$ stress, *Macellibacteroides* were enriched in the unclassified flora and became more dominant[53]. This implies that the difference in the bacterial community in this study might be caused by $Na^+$ in the hydrothermal-alkaline pretreatment. Hydrolytic and acid-producing bacteria are more adaptive than others and hence the reduction in biodiversity.

Figure 8c and d show microbial analysis of archaea at the phylum and genus levels. Euryarchaeota (46.5%), Halobacterota (42.1%), and Crenarchaeota (9.4%) were found the dominant archaea in the inoculum at the phylum level. Euryarchaeota (96.8% and 67.3%) and Halobacterota (3.2% and 32.6%) were the only two phyla detected in T_1 and T_2. At the genus level, *Methanosaeta* (39.7%) was the most abundant in the inoculum, followed by *Candidatus_Methanofastidiosum* (19.9%) and *Methanobrevibacter* (16.8%). *Methanosaeta* is an obligate acetoclastic methanogen that can produce acetyl-CoA from acetic acid and result in the production of an equal mole of $CO_2$ and $CH_4$[54]. On the contrary, only two genera i.e. *Methanobacterium* (96.8% and 67.3%) and *Methanosarcina* (3.2% and 32.6%), both of which are methanogens, were found in T_1 and T_2. *Methanobacterium* is a hydrogenotrophic methanogen and *Methanosarcina* is a mixed-trophic methanogen that is versatile in utilizing a variety of substrates including methyl-bearing compounds, hydrogen, and acetate for methane production[55,56]. The archaea community was overwhelmed by *Methanobacterium*, particularly in T_1, suggesting it was the major player in methane production.

Overall, the results indicate that the diversity of bacteria and archaea was reduced in the treated samples compared to the original inoculum, with hydrolytic and acid-producing bacteria being more adaptive and thus more prevalent.

## Discussion

The observed darkening color of the algal solution during pretreatment can be related to the Maillard reaction in the pretreatment system[57]. This reaction, which consumes dissolved proteins and carbohydrates, is thermodynamically favorable at high reaction temperatures (70 ~ 180 °C) and strong alkaline conditions[58]. This could well explain why the COD values were lower for hydrothermal-alkaline than hydrothermal pretreatment because of the presence of NaOH (Fig. 1). In addition, the hydrothermal-alkaline condition could significantly promote the Maillard reaction, producing by-products such as melanoidins from reducing sugars and proteins[59]. Overall, hydrothermal pretreatment was more effective than hydrothermal-alkaline pretreatment with respect to COD.

The surface morphology and structure of bloom algae biomass can undergo changes after pretreatment and microbial attacks (Fig. 5). Hydrothermal pretreatment tends to break weak chemical bonds such as hydrogen bonds on the surface of the algal cells. The dissolution of the extracellular polymeric substances can cause the lysis of cells that results in partial dissolution and exhibits in shattered fragments[60]. In hydrothermal-alkaline pretreatment, in addition to cell lysis, saponification reactions also occur, breaking down the components of cell walls and membranes (including cellulose and hemicellulose) and reducing the extent of fiber crystallinity[17]. After biodegradation, the roughness of algae increased further, forming honeycomb-like structures with numerous holes on the surface. This implies intensive microbial attacks during methane production. The increases in porous structure and roughness after pretreatment may increase the specific surface area of the biomass, especially in the hydrothermal-alkaline pretreatment, highlighting the importance of alkali in this process. As a result, the accessibility of algal biomass to microbial attachment and attacks can be greatly increased[61]. Concomitantly, the biodegradation further changes the structure of the biomass and enhances the dissolution of the inclusions in the algae cells and hence the increase in gas production.

*Klebsiella* is a crucial microbe in fermentation-based industries, known for its ability to effectively hydrolyze a variety of monosaccharides and disaccharides to produce $H_2$ and succinic acid, with glucose being the most efficient substrate[51,62,63]. This microbe can also utilize acetic acid, furfural, and 5-hydroxymethylfurfural as substrates[64,65]. The Maillard reaction of proteins and sugars at high temperatures can produce fermentation inhibitors, including 5-hydroxymethylfurfural, which is a favorable product in alkaline environments[59].

The FT-IR analysis (Fig. 6) has shown a C=O structure at 1651 $cm^{-1}$, which can be consolidated to 5-hydroxymethylfurfural C=O[38,39]. The intensity of the peaks of pretreatments was higher than the control, implying the formation of 5-hydroxymethylfurfural, which *Klebsiella* can convert to furoic acid and eventually to 2-oxy-glutaric acid, participating in the tricarboxylic acid cycle[66]. The intensity of the peaks in the treated samples decreased after incubation, corresponding to the increased abundance of *Klebsiella*. This observation may explain why methane production with bloom algae biomass treated with high temperature was not inhibited significantly in the microcosms.

After pretreatment, the pH of controls, hydrothermal pretreatment, and hydrothermal-alkaline pretreatment were 5.7, 5.2, and 8.7. The production of VFAs has contributed to the acidity of the samples while in the hydrothermal-alkaline pretreatment, the excess NaOH served as a neutralizing agent to increase the pH to above 7. Although the decomposition temperatures of formic acid, oxalic acid, and malic acid are high (306.8, 190, and 180 °C), the acid condition may facilitate the decomposition of some VFAs[63,67]. However, VFAs with low boiling temperatures may be lost due to volatilization in high-treatment temperatures (100 and 150 °C). On the other hand, the condition of hydrothermal-alkaline pretreatment was not conducive to the decomposition of chemically unstable VFAs due to its elevated pH.

Both treated samples also contained formic and acetic acids, which are direct substrates for methanogenesis (Fig. 7). This may have facilitated the reduction in lag time in gas production. After 20 days of incubation, all eight VFAs were detected in microcosms of control and hydrothermal pretreatment. This was due to the degradation of carbohydrates and other algal biomass[68]. Whereas, in the microcosms with hydrothermal-alkaline pretreatment, some VFAs including lactic, tartaric, and succinic acids were not detected throughout the incubation. In general, VFAs with high carbon numbers were not detected or present in low concentration upon the termination of incubation while low-carbon-number intermediates such as formic and acetic acids were found accumulated. This was not anticipated and the reason for this accumulation is unclear. Pearson correlation analysis revealed that there was a strong negative correlation between methane production and the total concentration of formic, acetic, and oxalic acids ($\rho$=-0.925). The concentrations of these acids were lower in the hydrothermal-alkaline pretreatment sample, suggesting the treatment has advantages over hydrothermal-only treatment in methane production.

Another factor that could account for the high methane yield in hydrothermal-alkaline pretreatment is the concentration of $Na^+$. Previous studies have reported that an increase in $Na^+$ concentration within a certain range can promote the growth of acetoclastic methanogens and increase methane production[69,70]. The carryover $Na^+$ from hydrothermal-alkaline pretreatment was found to be beneficial for the growth of *Methanosarcina* using acetic acid for methane production[71], as inferred by its high abundance in the microcosms (Fig. 9d). Its continuous consumption of acetic acid has mitigated the accumulation of acids and slowed down the pH drop which can reduce methane production. This agrees well with the VFAs analysis and gas production.

Studies have shown that algae could be used to produce methane reliably[72]. However, there are challenges associated with production. For instance, pH levels can affect the gas production from algae, but the adverse effects can be reduced by adjusting the pH with a buffering agent. In addition, the process of utilizing bloom algae for methane production involves energy-intensive heat treatment. Studies have shown that algae can be treated at 100 °C for 1 h for cost-saving purposes on an industrial-scale[73]. In this study, the pretreatment condition of 0.1 mol/L NaOH, 30 min, 100 °C is within the range and has also been shown to improve methane yields by as much as 237.5%. In terms of the acquisition of bloom algae, there are two main types of cultivation methods[72]. The first involves utilizing open ponds for bloom algae cultivation, benefitting from their rapid growth rate and higher economic returns. The second method employs photobioreactors for the cultivation. Considering the significant biomass requirements for production and application, the primary focus can be on using bloom algae from lakes, supplemented with open-air pond cultures. This approach not only fulfills our gas production needs but also addresses the pressing issue of water bloom pollution, maintaining a balanced water environment and preserving biodiversity[74].

## Conclusions

The present study evaluated the effectiveness of hydrothermal pretreatment and hydrothermal-alkaline pretreatment in enhancing methane production from bloom algae. In a 69-day gas production experiment, the effects of pretreatment conditions on methane production by anaerobic fermentation of bloom algae were investigated, and the changes of liquid components as well as structural changes in solids were analyzed. The results indicate that both pretreatments can increase methane yields, but to various degrees. The most effective conditions were found to be the use of 0.2 mol/L NaOH and heating at 150 °C for 30 min, resulting in a 303% increase in methane production. Analyses have shown that both hydrothermal pretreatment and hydrothermal-alkaline pretreatment can effectively alter the cell structure of the bloom algae and promote the dissolution of intracellular carbohydrates and other substances. Additionally, an appropriate increase in the concentration of NaOH in the hydrothermal-alkaline pretreatment can reduce the loss of VFAs during the pretreatment process and slow down the decrease of pH, which is beneficial to methane production. These results indicate that hydrothermal-alkaline pretreatment offers significant advantages in methane production compared to hydrothermal pretreatment. The findings in this study have implications for utilizing bloom algae as a source for the production of renewable natural gas.

## Data availability

Data is provided within the manuscript or supplementary information files.

Received: 10 March 2024; Accepted: 10 February 2025

Published online: 25 February 2025

## References


1. Gaedicke, C. et al. *Federal Institute Geosci Nat Resour, Hannover, Germany* (2022).
2. Huang, Z. et al. Removal of ions from produced water using Powder River Basin coal. *Int. J. Coal Sci. Technol.* **9**, 1 (2022).
3. Barnhart, E. P. et al. Enhanced coal-dependent methanogenesis coupled with algal biofuels: potential water recycle and carbon capture. *Int. J. Coal Geol.* **171**, 69–75 (2017).
4. Huang, Z. et al. Low carbon renewable natural gas production from coalbeds and implications for carbon capture and storage. *Nat. Commun.* **8**, 568 (2017).
5. Smith, H. J. et al. Effect of an algal amendment on the microbial conversion of coal to methane at different sulfate concentrations from the Powder River Basin, USA. *Int. J. Coal Geol.* **248**, 103860 (2021).
6. Wu, H. et al. Mechanisms and enhancements on harmful algal blooms conversion to bioenergy mediated with dual-functional chitosan. *Appl. Energy*. **327**, 120142 (2022).
7. Wang, S., Diao, X. & He, L. Effects of algal bloom formation, outbreak, and extinction on heavy metal fractionation in the surficial sediments of Chaohu Lake. *Environ. Sci. Pollut. Res.* **22**, 14269–14279 (2015).
8. Sun, R., Sun, P., Zhang, J., Esquivel-Elizondo, S. & Wu, Y. Microorganisms-based methods for harmful algal blooms control: a review. *Bioresour. Technol.* **248**, 12–20 (2018).
9. Sainju, U. M. & Allen, B. L. Carbon footprint of perennial bioenergy crop production receiving various nitrogen fertilization rates. *Sci. Total Environ.* **861**, 160663 (2023).
10. Bibi, F., Jamal, A., Huang, Z., Urynowicz, M. & Ali, M. I. Advancement and role of abiotic stresses in microalgae biorefinery with a focus on lipid production. *Fuel* **316**, 123192 (2022).
11. Tazikeh, S., Zendehboudi, S., Ghafoori, S., Lohi, A. & Mahinpey, N. Algal bioenergy production and utilization: technologies, challenges, and prospects. *J. Environ. Chem. Eng.* 107863 (2022).
12. Jankowska, E., Sahu, A. K. & Oleskowicz-Popiel, P. Biogas from microalgae: review on microalgae's cultivation, harvesting and pretreatment for anaerobic digestion. *Renew. Sustain. Energy Rev.* **75**, 692–709 (2017).
13. Ward, A., Lewis, D. & Green, F. Anaerobic digestion of algae biomass: a review. *Algal Res.* **5**, 204–214 (2014).
14. Carrère, H. et al. Pretreatment methods to improve sludge anaerobic degradability: a review. *J. Hazard. Mater.* **183**, 1–15 (2010).
15. Alzate, M., Muñoz, R., Rogalla, F., Fdz-Polanco, F. & Pérez-Elvira, S. Biochemical methane potential of microalgae: influence of substrate to inoculum ratio, biomass concentration and pretreatment. *Bioresour. Technol.* **123**, 488–494 (2012).
16. Bai, X., Lant, P. A., Jensen, P. D., Astals, S. & Pratt, S. Enhanced methane production from algal digestion using free nitrous acid pre-treatment. *Renew. Energy*. **88**, 383–390 (2016).
17. Bohutskyi, P., Betenbaugh, M. J. & Bouwer, E. J. The effects of alternative pretreatment strategies on anaerobic digestion and methane production from different algal strains. *Bioresour. Technol.* **155**, 366–372 (2014).
18. Saleem, S., Ullah, Z., Rashid, N. & Sheikh, Z. Effect of hydrothermal pretreatment on leachate fed Scenedesmus sp. biomass solubilization and biogas production. *J. Environ. Manage.* **365**, 121515 (2024).
19. Passos, F., Uggetti, E., Carrère, H. & Ferrer, I. Pretreatment of microalgae to improve biogas production: a review. *Bioresour. Technol.* **172**, 403–412 (2014).
20. Tian, C., Li, B., Liu, Z., Zhang, Y. & Lu, H. Hydrothermal liquefaction for algal biorefinery: a critical review. *Renew. Sustain. Energy Rev.* **38**, 933–950 (2014).
21. Babu, R., Capannelli, G., Bernardini, M., Pagliero, M. & Comite, A. Effect of varying hydrothermal temperature, time, and sludge pH on sludge solubilisation. *Carbon Resour. Convers.* **6**, 142–149 (2023).
22. Wu, H., Huang, S., Wang, K. & Liu, Z. Coproduction of amino acids and biohythane from microalgae via cascaded hydrothermal and anaerobic process. *Sci. Total Environ.* **872**, 162238 (2023).
23. Otite, S. V. et al. Effect of the Inoculum-to-substrate ratio on putative pathogens and Microbial Kinetics during the batch anaerobic digestion of simulated Food Waste. *Microorganisms* **12**, 603 (2024).
24. Mansour, M. N. et al. Influence of substrate/inoculum ratio, inoculum source and ammonia inhibition on anaerobic digestion of poultry waste. *Environ. Technol.* **45**, 1894–1907 (2024).
25. Rodriguez, C., Alaswad, A., Mooney, J., Prescott, T. & Olabi, A. Pre-treatment techniques used for anaerobic digestion of algae. *Fuel Process. Technol.* **138**, 765–779 (2015).
26. Leite, W. R. M. et al. Mesophilic anaerobic digestion of waste activated sludge in an intermittent mixing reactor: Effect of hydraulic retention time and organic loading rate. *J. Environ. Manage.* **338**, 117839 (2023).
27. Liu, X., Liu, J. & Fang, J. Frost-heave characteristics of saturated lean clay fillers by orthogonal test design considering the static surcharge. *Case Stud. Constr. Mater.* **17**, e01526 (2022).
28. Aftab, T., Landi, M., Papadakis, I. E., Araniti, F. & Brown, P. H. *Boron in Plants and Agriculture: Exploring the Physiology of Boron and Its Impact on Plant Growth* (Academic, 2022).
29. Wei, C. et al. Residual chemical oxygen demand (COD) fractionation in bio-treated coking wastewater integrating solution property characterization. *J. Environ. Manage.* **246**, 324–333 (2019).
30. He, H. et al. Microbial community succession between coal matrix and culture solution in a simulated methanogenic system with lignite. *Fuel* **264**, 116905 (2020).
31. Li, L. et al. Biogas production potential and kinetics of microwave and conventional thermal pretreatment of grass. *Appl. Biochem. Biotechnol.* **166**, 1183–1191 (2012).
32. Claesson, M. J. et al. Comparative analysis of pyrosequencing and a phylogenetic microarray for exploring microbial community structures in the human distal intestine. *PloS One*. **4**, e6669 (2009).
33. Zhang, Y. et al. In-situ mineral CO2 sequestration in a methane producing microbial electrolysis cell treating sludge hydrolysate. *J. Hazard. Mater.* **394**, 122519 (2020).
34. Passos, F., Felix, L., Rocha, H., de Oliveira Pereira, J. & de Aquino, S. Reuse of microalgae grown in full-scale wastewater treatment ponds: thermochemical pretreatment and biogas production. *Bioresour. Technol.* **209**, 305–312 (2016).
35. Sun, C. et al. Improving production of volatile fatty acids and hydrogen from microalgae and rice residue: effects of physicochemical characteristics and mix ratios. *Appl. Energy*. **230**, 1082–1092 (2018).
36. Cheng, J. et al. Physicochemical characterization of typical municipal solid wastes for fermentative hydrogen and methane co-production. *Energy. Conv. Manag.* **117**, 297–304 (2016).
37. Rodríguez-Abalde, Á. et al. Study of thermal pre-treatment on anaerobic digestion of slaughterhouse waste by TGA-MS and FTIR spectroscopy. *Waste Manag. Res.* **31**, 1195–1202 (2013).
38. Armaroli, T. et al. Acid sites characterization of niobium phosphate catalysts and their activity in fructose dehydration to 5-hydroxymethyl-2-furaldehyde. *J. Mol. Catal. A: Chem.* **151**, 233–243 (2000).
39. Zhao, K. et al. Fabrication of – SO3H functionalized aromatic carbon microspheres directly from waste Camellia oleifera shells and their application on heterogeneous acid catalysis. *Mol. Catal.* **433**, 193–201 (2017).
40. Solymosi, F. & Zakar, T. S. FT-IR study on the interaction of CO2 with H2 and hydrocarbons over supported re. *J. Mol. Catal. A: Chem.* **235**, 260–266 (2005).
41. Han, Y. et al. Circular dichroism and infrared spectroscopic characterization of secondary structure components of protein Z during mashing and boiling processes. *Food Chem.* **188**, 201–209 (2015).

42. Chen, C. et al. Sustainable biohythane production from algal bloom biomass through two-stage fermentation: impacts of the physicochemical characteristics and fermentation performance. *Int. J. Hydrog. Energy*. **45**, 34461–34472 (2020).
43. Dong, W. et al. Caproic acid production from anaerobic fermentation of organic waste-pathways and microbial perspective. *Renew. Sustain. Energy Rev.* **175**, 113181 (2023).
44. Qiu, W. et al. Aerobic composting of chicken manure with Amoxicillin: alpha diversity is closely related to lipid metabolism, and two-component systems mediating their relationship. *Bioresour. Technol.* **360**, 127543 (2022).
45. Too, C. C., Ong, K. S., Yule, C. M. & Keller, A. Putative roles of bacteria in the carbon and nitrogen cycles in a tropical peat swamp forest. *Basic Appl. Ecol.* **52**, 109–123 (2021).
46. Zuo, X. et al. The relationships among sCOD, VFAs, microbial community, and biogas production during anaerobic digestion of rice straw pretreated with ammonia. *Chin. J. Chem. Eng.* **28**, 286–292 (2020).
47. Kim, B. C. et al. Caproiciproducens galactitolivorans gen. nov., sp. nov., a bacterium capable of producing caproic acid from galactitol, isolated from a wastewater treatment plant. *Int. J. Syst. Evol. MicroBiol.* **65**, 4902–4908 (2015).
48. Tang, J. et al. Caproate production from xylose via the fatty acid biosynthesis pathway by genus Caproiciproducens dominated mixed culture fermentation. *Bioresour. Technol.* **351**, 126978 (2022).
49. Li, B. Y. et al. Production of volatile fatty acid from fruit waste by anaerobic digestion at high organic loading rates: performance and microbial community characteristics. *Bioresour. Technol.* **346**, 126648 (2022).
50. Jeong, S. Y. & Kim, T. G. Determination of methanogenesis by nutrient availability via regulating the relative fitness of methanogens in anaerobic digestion. *Sci. Total Environ.* **838**, 156002 (2022).
51. Niu, K., Zhang, X., Tan, W. S. & Zhu, M. L. Characteristics of fermentative hydrogen production with Klebsiella pneumoniae ECU-15 isolated from anaerobic sewage sludge. *Int. J. Hydrog. Energy*. **35**, 71–80 (2010).
52. Chen, Y., Yin, Y. & Wang, J. Influence of butyrate on fermentative hydrogen production and microbial community analysis. *Int. J. Hydrog. Energy*. **46**, 26825–26833 (2021).
53. Fang, W., Yang, Y., Wang, C. & Zhang, P. Enhanced volatile fatty acid production from anaerobic fermentation of waste activated sludge by combined sodium citrate and heat pretreatment. *J. Environ. Chem. Eng.* **10**, 108518 (2022).
54. Welte, C. & Deppenmeier, U. Bioenergetics and anaerobic respiratory chains of aceticlastic methanogens. *Biochim. et Biophys. Acta (BBA)-Bioenergetics*. **1837**, 1130–1147 (2014).
55. Zhang, W., Zhang, F., Li, Y. X., Jiang, Y. & Zeng, R. J. No difference in inhibition among free acids of acetate, propionate and butyrate on hydrogenotrophic methanogen of Methanobacterium formicicum. *Bioresour. Technol.* **294**, 122237 (2019).
56. Basak, B. et al. Syntrophic bacteria-and Methanosarcina-rich acclimatized microbiota with better carbohydrate metabolism enhances biomethanation of fractionated lignocellulosic biocomponents. *Bioresour. Technol.* **360**, 127602 (2022).
57. Shakoor, A., Zhang, C., Xie, J. & Yang, X. Maillard reaction chemistry in formation of critical intermediates and flavour compounds and their antioxidant properties. *Food Chem.* 133416 (2022).
58. Lotfy, S. N., Saad, R., El-Massrey, K. F. & Fadel, H. H. Effects of pH on headspace volatiles and properties of Maillard reaction products derived from enzymatically hydrolyzed quinoa protein-xylose model system. *LWT* **145**, 111328 (2021).
59. Bork, L. V., Haase, P. T., Rohn, S. & Kanzler, C. Structural characterization of polar melanoidins deriving from Maillard reaction intermediates–A model approach. *Food Chem.* **395**, 133592 (2022).
60. Passos, F., García, J. & Ferrer, I. Impact of low temperature pretreatment on the anaerobic digestion of microalgal biomass. *Bioresour. Technol.* **138**, 79–86 (2013).
61. Li, S. et al. Experimental study on the change of coal structure and microbial community structure during supercritical-CO2-H2O-microorganisms-coal interaction process. *Environ. Technol. Innov.* 103036 (2023).
62. Cheng, K. K. et al. Effects of pH and dissolved CO2 level on simultaneous production of 2, 3-butanediol and succinic acid using Klebsiella pneumoniae. *Bioresour. Technol.* **135**, 500–503 (2013).
63. Varghese, V. K., Poddar, B. J., Shah, M. P., Purohit, H. J. & Khardenavis, A. A. A comprehensive review on current status and future perspectives of microbial volatile fatty acids production as platform chemicals. *Sci. Total Environ.* 152500 (2021).
64. Parate, R. D., Dharne, M. S. & Rode, C. V. Integrated chemo and bio-catalyzed synthesis of 2, 5-furandicarboxylic acid from fructose derived 5-hydroxymethylfurfural. *Biomass Bioenerg.* **161**, 106474 (2022).
65. Ra, C. H., Jeong, G. T., Shin, M. K. & Kim, S. K. Biotransformation of 5-hydroxymethylfurfural (HMF) by Scheffersomyces stipitis during ethanol fermentation of hydrolysate of the seaweed Gelidium amansii. *Bioresour. Technol.* **140**, 421–425 (2013).
66. Koopman, F., Wierckx, N., de Winde, J. H. & Ruijssenaars, H. J. Identification and characterization of the furfural and 5-(hydroxymethyl) furfural degradation pathways of Cupriavidus basilensis HMF14. *Proc. Natl. Acad. Sci. USA* **107**, 4919–4924 (2010).
67. Federico, B. et al. New insights in food waste, sewage sludge and green waste anaerobic fermentation for short-chain volatile fatty acids production: a review. *J. Environ. Chem. Eng.* 108319 (2022).
68. Liu, F. et al. Characterization of organic compounds from hydrogen peroxide-treated subbituminous coal and their composition changes during microbial methanogenesis. *Fuel* **237**, 1209–1216 (2019).
69. Roy, C. K. et al. Effect of sodium tungstate on anaerobic digestion of waste sewage sludge: enhanced methane production via increased acetoclastic methanogens. *J. Environ. Chem. Eng.* **10**, 107524 (2022).
70. Gagliano, M. C., Sudmalis, D., Temmink, H. & Plugge, C. M. Calcium effect on microbial activity and biomass aggregation during anaerobic digestion at high salinity. *New Biotechnol.* **56**, 114–122 (2020).
71. Lee, J., Kim, E. & Hwang, S. Effects of inhibitions by sodium ion and ammonia and different inocula on acetate-utilizing methanogenesis: methanogenic activity and succession of methanogens. *Bioresour. Technol.* **334**, 125202 (2021).
72. Jabłońska-Trypuć, A. et al. Using algae for biofuel production: a review. *Energies* **16**, 1758 (2023).
73. Zieliński, M. et al. The effect of pressure and temperature pretreatment on the biogas output from algal biomass. *Environ. Technol.* **36**, 693–698 (2015).
74. Guan, M. et al. Quantifying the effects of wind wave on Cyanobacterial blooms in large shallow lake from 10 years high frequency satellite observation. *Hydrobiologia* 1–18 (2024).


## Acknowledgements

This work was supported by Fundamental Research Funds for the Central Universities of China [2021ZDPY0210] & [2022ZZCX01K1], National Key Research and Development Program of China [2021YFC2902603], National Key Research and Development Program of China [2019YFC1805400], National Natural Science Foundation of China [No. 42172187], Key Research Development Program of in Modern Agriculture [KC21137].

## Author contributions

Zaixing Huang: Conceptualization, Methodology, Investigation, Resources, Data Curation, Writing - Original Draft, Writing - Review & Editing, Visualization, Supervision, Project administration, Funding acquisition-Jingzhuo Zhou: Yuxiang Zhong: Validation, Formal analysis, Investigation, Data Curation, Writing - Review & EditingYuxiang Zhong: Validation, Formal analysis, Investigation, Data Curation, Writing - Original Draft, Writing - Review & EditingYajie Chang: Validation, Formal analysis, Investigation, Data CurationWanrong Yin:

Zhong: Validation, Formal analysis, Investigation, Data CurationShuzhong Zhao: Validation, Formal analysis, InvestigationYi Yan: Validation, Formal analysis, InvestigationWeting Zhang: Validation, Formal analysis, Writing - Review & EditingQingfeng Gu: Investigation, Data Curation, Writing - Original DraftHuan He: Methodology, Investigation, Resources, Writing - Review & Editing, Supervision, Project administration, Funding acquisitionMichael Urynowicz: Writing - Review & EditingMuhammad Adnan Sabar: Writing - Review & EditingGordana Medunić: Writing - Review & EditingFang-Jing Liu: Writing - Data Curation, Review & Editing-Hongguang Guo: Writing - Review & EditingAsif Jamal: Writing - Review & EditingMuhammad Ishtiaq Ali: Writing - Review & EditingRizwan Haider: Writing - Review & Editing.

## Declarations

## Competing interests
The authors declare no competing interests.

## Additional information
**Correspondence** and requests for materials should be addressed to Z.H. or H.H.

**Reprints and permissions information** is available at www.nature.com/reprints.

**Publisher's note** Springer Nature remains neutral with regard to jurisdictional claims in published maps and institutional affiliations.